Applied Radiation and Isotopes 192 (2023) 110612

Contents lists available at ScienceDirect

Applied Radiation and Isotopes

journal homepage: www.elsevier.com/locate/apradiso

Improved procedures for production and purification of ^{135}La from enriched [^{135}Ba]$BaCO_3$ on a 16.5 MeV cyclotron

Kristina Søborg Pedersen [a,1], Claire Deville [a,1], Ursula Søndergaard [b,c], Mikael Jensen [a,**], Andreas I. Jensen [a,*]

[a] The Hevesy Laboratory, Department of Health Technology, Technical University of Denmark, Frederiksborgvej 399, Building 202, 4000, Roskilde, Denmark
[b] University Hospital of North Norway, Sykehusvegen 38, 9019, Tromsø, Norway
[c] Arctic University of Norway, Hansine Hansens veg 18, 9019, Tromsø, Norway

ARTICLE INFO

Keywords:
Lanthanum-135
Auger electron radiotherapy
Proton irradiation
Cyclotron target
Purification
Radiolabeling

ABSTRACT

Lanthanum-135 (^{135}La) is a favorable Auger electron emitter with a high Auger electron yield and low gamma emission, making it promising for Auger electron radiotherapy. However, successful application requires reliable and scalable ^{135}La production. Up to now, metallic natural barium (^{nat}Ba) is a commonly used target material, but this material is sensitive to moisture and oxidation. $BaCO_3$ has also been tested, due to its higher chemical stability. However, $BaCO_3$ has poor thermal conductivity, limiting the applicable current and making high yield production challenging. In this study, we pressed a mixture of enriched [^{135}Ba]$BaCO_3$ and fine aluminum (Al) powder to provide a stable target with improved thermal conductivity compared to pure $BaCO_3$. After 4 h of irradiation with a 16.5 MeV proton beam at 20 μA current, 1.62 ± 0.18 GBq was produced from a 200 mg [^{135}Ba]$BaCO_3$:Al (1:2, w/w) target. This corresponded to a saturation yield of 11.91 ± 1.31 GBq (or 596 ± 66 MBq/μA). A purification procedure involving initial precipitation, followed by a single composite column containing a layer of TK200 resin and a second layer of branched DGA resin was developed, with 97.1 ± 3.6 % decay corrected ^{135}La recovery. [^{135}La]$LaCl_3$ was obtained in an effective molar activity of 79.6 ± 25.3 MBq/nmol (DOTA titration), 104.0 ± 40.4 MBq/nmol (DTPA titration) and 186.5 ± 83.8 MBq/nmol (CHX-A″-DTPA titration), and a radionuclidic purity (RNP) of >99.9 % at end of purification, hereby demonstrating a purity suitable for radiopharmaceutical use.

1. Introduction

Auger electron radiotherapy (AeRT) utilizes radionuclides that emit cascades of low energy electrons (<25 keV) upon decay by electron capture or isomeric transition (Ku et al., 2019). The linear energy transfer (LET) for Auger electrons is around 4–26 keV/μm, meaning that the energy is deposited within a very short tissue range. This makes AeRT favorable for a highly accurate therapy, targeting cancer cell nuclei, with low off-target damage (Álvarez et al., 2021). A variety of Auger emitting radionuclides with favorable properties for AeRT exist. The production of the radionuclide is an important factor for the potential use of the radionuclide in clinical applications since sufficient amounts and purity are needed. Furthermore, the labeling of suitable targeting vectors with the radionuclide must be developed in order to deliver the radionuclide to or close to the targeted cell nuclei (Filosofov et al., 2021). ^{135}La has been attracting increasing attention during recent years due to its favorable properties for AeRT. ^{135}La decays to stable ^{135}Ba by electron capture with a half-life of 18.91 h (Abel et al., 2018). It is a suitable Auger emitter with an average of 10.9 electrons emitted per decay (Fonslet et al., 2018) and with limited other emissions, most notably one γ photon at 480.51 keV (1.52%), and β^+ annihilation photons at 511 keV (0.014%) and X-ray emissions between 4.5 and 37.3 keV (84.3 %). These properties make ^{135}La a highly promising candidate for AeRT (Buchegger et al., 2006). The chemical properties are also favorable as La(III) forms stable complexes with the widely used 1,4,7,10-tetraazacyclododecane-1,4,7,10-tetraacetic acid (DOTA) chelator (Viola-Villegas and Doyle, 2009). This simplifies the implementation of ^{135}La in the development of radiopharmaceuticals as currently know

* Corresponding author.
** Corresponding author.
E-mail addresses: kmje@dtu.dk (M. Jensen), atije@dtu.dk (A.I. Jensen).
[1] These 2 authors have contributed equally to the study.

https://doi.org/10.1016/j.apradiso.2022.110612
Received 19 September 2022; Received in revised form 19 November 2022; Accepted 8 December 2022
Available online 8 December 2022

targeting vectors conjugated to DOTA can be used.

^{135}La production on cyclotrons has been reported by several research laboratories through the past years. In most cases, pressed ^{nat}Ba was used as target material. ^{nat}Ba contains a mixture of six stable Ba isotopes: ^{132}Ba (0.1%), ^{134}Ba (2.4%), ^{135}Ba (6.6%), ^{136}Ba (7.9%), ^{137}Ba (11.2%), and ^{138}Ba (71.7%). Bombardment of ^{nat}Ba therefore results in a mixture of La isotopes. The commonly observed La radioisotopes produced by cyclotron bombardment of ^{nat}Ba are ^{132}La, ^{133}La, and ^{135}La. In 2018, Fonslet et al. reported a procedure in which they reached a saturation yield of 407 MBq/μA for ^{135}La and an effective molar activity of 70 MBq/nmol after purification on a CM cation exchange resin (Fonslet et al., 2015, 2018). In this report, the Auger electron cascade was calculated to give on average 10.6 very low energy electrons per decay, which have energies below 4 keV. Abel et al. produced ^{135}La and ^{132}La in order to precisely measure their half-lives (Abel et al., 2018). Pressed metallic ^{nat}Ba was again used as target material and the purification was performed on a column packed with DGA resin. The same target material and a similar purification method were applied by Aluicio-Sarduy et al. (2019) in the production of the theranostic pair ^{132}La/^{135}La. Two different irradiation conditions were tested and it was observed that irradiation at 16 MeV/25 μA produced a better ^{135}La yield, albeit with lower radionuclidic purity due to the production of proportionally higher amounts of ^{133}La ($T_{½}$ = 3.91 h) compared to irradiation at 11.9 MeV/10 μA. After the purification, an effective molar activity of 22 MBq/nmol was measured. The study also reported the biodistribution of unchelated La, which was found to essentially accumulate in the liver and bones. The same research group produced the pair ^{132}La/^{135}La again one year later (Aluicio-Sarduy et al., 2020) with focus on chelation chemistry and potential medical applications of the radionuclides, investigated in a murine PSMA expressing prostate cancer model. Metallic ^{nat}Ba has the drawback of being very sensitive to moisture and oxidation, which affects the chemical composition and thereby the physical properties such as thermal conductivity and melting point of the target. To address this problem, Nelson et al. (Nelson et al., 2020, 2022) reported a ^{nat}Ba target sealed with a 25 μm Al foil, and stored under argon atmosphere. Irradiation with a proton beam at 22 MeV produced the pair ^{133}La/^{135}La with saturation yields of 161 MBq/μA and 561 MBq/μA, respectively. After purification on DGA resin, the resulting effective molar activities were 33 MBq/nmol for ^{133}La and 47 MBq/nmol for ^{135}La. In the same paper, cross sections for the proton-induced nuclear reactions on $^{132/134/135/136/137}$Ba to make $^{132/133/135}$La were simulated and reported. Recently, Nielsen & Jensen produced ^{135}La from metallic ^{nat}Ba and used the LN resin in an effective and rapid purification procedure (Nielsen and Jensen, 2021).

Pressed $^{nat}BaCO_3$ (Jastrzębski et al., 2020; Chakravarty et al., 2022) and enriched [^{135}Ba]$BaCO_3$ (Mansel and Franke, 2015; Nelson et al., 2022) have also been reported as suitable target materials. The activities produced were low however, likely due to the necessity of applying only low current during the bombardment (less than 10 μA). $BaCO_3$ has a lower thermal conductivity than metallic Ba and target decomposition may occur at higher currents. $BaCO_3$ also presents the drawback of being difficult to press in pure form as it is significantly harder than silver ($BaCO_3$ 3.5 Mohs vs Ag 2.5 Mohs), excluding the use of silver as target supports.

In this report, we describe two separate improvements to the production and purification of ^{135}La. The first pertains to target composition. We report the use of a combination of enriched [^{135}Ba]$BaCO_3$ and fine Al powder as target material. This allows for the production of ^{135}La at higher beam currents and thus higher activities without the presence of other La radioisotopes arising from the irradiation of a ^{nat}Ba target. Further, a higher current can be used compared to a pure [^{135}Ba]$BaCO_3$ target, as the presence of Al leads to better heat conduction and makes the target stable during irradiation at up to 20 μA. The second improvement is the use of a mixture of branched DGA resin and TK200 resin in the purification procedure. This makes it possible to obtain ^{135}La of adequate chemical and radionuclidic purity after a simple purification procedure, despite the substantial amounts of Al and trace metal impurities present in the target.

2. Experimental part

2.1. Material and methods

All chemicals were purchased from Sigma-Aldrich unless otherwise noted, and used without further purification. [^{135}Ba]$BaCO_3$ (94.9 % enrichment) was purchased from CortecNet SA. Al powder (99.9 %, 60 μm max. particle size) and Nb foil (99.9 %, 50 μm thickness) were purchased from Goodfellow. Water was of 18 MΩ MilliQ-grade. The TK200 resin was purchased from TrisKem and DGA resin (branched) was purchased from TrisKem or from Eichrom Technologies Inc. DOTA and *p*-NO_2-Bn-CHX-A″-DTPA were purchased from Macrocyclics. Mouse serum was purchased from Biowest. TLC Silica gel 60 F_{254} plates (Aluminium sheets) were used for thin layer chromatography and purchased from Merck. A GE 16.5 MeV PETtrace cyclotron was used for the irradiations of the targets. The peristaltic pump was a BT100-2J LongerPump. Non-radioactive metal impurities in the final sample were quantified by ICP-OES using a Thermo Scientific iCAP 7000 Plus Series ICP-OES apparatus. The activities of the samples were measured using a Princeton Gammatech LGC 5 germanium detector Gamma spectrometer. For the effective specific activity measurements, the TLC plates were eluted with a 1:1 H_2O:MeOH mixture containing NH_4OAc (5%, w/v) and were read using a PerkinElmer Cyclone® Plus Storage Phosphor System apparatus.

2.2. Cyclotron production of ^{135}La from $^{nat}BaCO_3$

A homogeneous $^{nat}BaCO_3$:Al powder mixture (1:2, w/w, 150 mg) was pressed into a silver disc (28 mm × 5 mm) carved in the center (9 mm × 3 mm hole) with 0.5–1 t pressure using a hydraulic press. The disc was mounted into a target holder with direct water cooling on the backside of the silver disc. A 50 μm thick Nb foil was placed in front of the target. The target was irradiated with a 16.5 MeV proton beam at 10–20 μA for 30–120 min. The target was left overnight on the cyclotron before handling for short-lived isotopes to decay.

The same procedure was used for the target with a larger target diameter, where 361 mg $^{nat}BaCO_3$:Al powder mixture (1:2, w/w) was pressed into a silver disc (28 mm × 5 mm) carved in the center (14 mm × 3 mm hole) with 2.5 t pressure using a hydraulic press. The target was irradiated at 20 μA for 1 h.

The target with a higher $^{nat}BaCO_3$ content was prepared by pressing a homogeneous $^{nat}BaCO_3$:Al powder mixture (1:1, w/w, 150 mg) into a silver disc (28 mm × 5 mm) carved in the center (9 mm × 3 mm hole) with 0.5–1 t pressure using a hydraulic press and following the same procedure as for the $^{nat}BaCO_3$:Al (1:2, w/w) target. The target was irradiated at 20 μA for 1 h.

2.3. Cyclotron production of ^{135}La from [^{135}Ba]$BaCO_3$

[^{135}Ba]$BaCO_3$ (^{135}Ba enrichment 94.9%) was used in this procedure. The [^{135}Ba]$BaCO_3$:Al ratio was 1:2 (w/w) and the target preparation was the same as with $^{nat}BaCO_3$. 150–200 mg of the target material with a 9 mm target diameter was used. The target was irradiated with 16.5 MeV proton beam at 20 μA for 4 h. The target was left for 30 min on the cyclotron before handling for short-lived isotopes to decay.

2.4. ^{135}La purification (procedure for irradiated [^{135}Ba]$BaCO_3$ targets)

The target holder was dismounted, the Nb foil removed, and the silver disc was attached to a dissolution chamber. Portions of aq. HCl (3 M) were added until complete dissolution of the Al and $BaCO_3$ at 60 °C (total volume added: 9–11 mL). The target solution was evaporated to dryness at 130 °C under a stream of argon in a closed vial with argon

inlet and a wider diameter outlet to avoid contamination. The resulting solid was then taken up in aq. HCl (0.01 M, 1.5–1.75 mL) and this solution was transferred to a 15 mL centrifugal tube. Aq. HCl (30 % (w/w), 8–9 mL) was added and the mixture was left a few minutes to allow for $BaCl_2$ to precipitate. The mixture was centrifuged at 3000 rpm for 1 min and the supernatant was collected. The precipitate was extracted twice with aq. HCl (8 M, 2 mL), followed by centrifugation and collection of the supernatants. The combined supernatants were loaded on a 1 mL column filled with 100 mg TrisKem TK200 resin at the bottom and 300 mg TrisKem DGA resin (branched) on the top, previously washed with aq. HCl (3 M, 5 mL) and conditioned with aq. HCl (8 M, 5 mL). The column was washed with aq. HCl (8 M, 20 mL) using a peristaltic pump with a flow rate of 1 mL/min. The ^{135}La was then eluted with aq. HCl (3 M, 3 mL). The eluate was evaporated to dryness and reconstituted in aq. HCl (0.001 M, 0.2 mL). The product was analyzed by ICP-OES in order to quantify the remaining non-radioactive metal impurities. 10 μL of the product was diluted up to 5 mL with 1 % aq. HCl. Ba/La and Al/La separation factors were calculated from the distribution of the elements on the column. The distribution was calculated by dividing the amount of the element after the purification with the amount of the element before the purification subtracted the amount of the element after the purification. The separation factors were calculated by dividing the distribution of La with the distribution of Ba or Al.

2.5. Recycling of ^{135}Ba from $^{135}BaCl_2$ precipitate

The [^{135}Ba]$BaCl_2$ precipitate was dissolved in water (4–6 mL) and the solution was passed through a syringe filter. An aqueous solution of $(NH_4)_2CO_3$ (1.3 M, 6 mL) was added dropwise until full precipitation of the [^{135}Ba]$BaCO_3$ was obtained. The resulting suspension was centrifuged at 3000 rpm for 1 min and the supernatant was removed. The sample was washed twice, by addition of 5 mL water followed by centrifugation. After removal of the supernatant, the wet powder was transferred into a vial and dried at 130 °C under a stream of argon.

2.6. Effective molar activity determination

The effective molar activity was measured by titrating an aliquot of the final sample with DOTA, DTPA, or *p*-NO_2-Bn-CHX-A″-DTPA. 25–50 μL of the purified $^{135}LaCl_3$ solution (12.5–25% of total volume), was mixed with aq. NH_4OAc (0.03–0.1 M, 230 μL). Increasing amounts of aq. DOTA, DTPA or CHX-A″-DTPA (50 μM) in aq. NH_4OAc (0.1 M) were then added. First, 10–20 μL of chelator solution was added (0.5–1 nmol chelator), followed by 30 min heating at 90 °C for DOTA and 30 min at room temperature for DTPA and CHX-A″-DTPA. The solutions were spotted on a TLC plate (normal phase). Then 4–5 successive additions of 10 μL (1, 1.5, 2, 2.5, 3 nmol) or 20 μL (2, 3, 4, 5, 6 nmol) chelator solution were performed. The TLC plates were eluted with a 1:1 H_2O:MeOH mixture containing NH_4OAc (5%, w/v). The ^{135}La-DOTA complex had an R_f of 0.3–0.4, the ^{135}La-DTPA an R_f of 0.6–0.7 and the ^{135}La-CHX-A″-DTPA an R_f of 0.8–0.9, while the non-chelated ^{135}La remained on the starting line. The amount of competing metals was calculated by dividing the amount of chelator added to the solution with the fraction of ^{135}La-complex formed. Only points with chelator complex formation below 100% were used for the calculations.

2.7. Serum stability of ^{135}La-DOTA, ^{135}La-DTPA and ^{135}La-CHX-A″-DTPA

50 μL of around 10 MBq of ^{135}La-DOTA, ^{135}La-DTPA, or ^{135}La-DTPA in aq. NH_4OAc (0.1 M), were mixed with mouse serum (1.0 mL). The mixtures were incubated at 37 °C. Samples were analyzed by radio-TLC (normal phase, eluent 1:1 H_2O:MeOH mixture containing 5% (w/v) NH_4OAc) at 0, 3, 18, 24, 42, and 48 h. The experiment was done in triplicate.

3. Results

3.1. Evaluation of ^{135}La production with a $^{nat}BaCO_3$:Al target

A $^{nat}BaCO_3$ based target was first developed, which would remain stable when exposed to a proton beam at 16.5 MeV and 20 μA, behind a 50 μm thick niobium (Nb) foil degrading the on-target beam energy to 15.8 MeV. An overview of the tested $^{nat}BaCO_3$:Al targets can be seen in Table 1. 150 mg of a 1:2 (w/w) mixture of $^{nat}BaCO_3$ and Al was pressed at 0.5–1 tons (780–1560 kg/cm^2) into a silver disc (28 mm × 5 mm) carved in the center (9 mm × 3 mm hole) (Table 1, Target 1). The targets pressed in this way presented a smooth, metallic, slightly shiny surface (Fig. 1A). A w/w ratio of 1:2 ($^{nat}BaCO_3$:Al) was found to be a suitable ratio for ensuring the stability under these conditions, while maintaining an appreciable ^{135}Ba content (Fig. 1B). Limited burnings could be observed on the surface of the 1:2 $^{nat}BaCO_3$:Al (w/w) target after 1 h of irradiation if the target pressing was imperfect and the target slightly cracked. This was likely due to a decrease in heat conductivity and decomposition of some of the carbonate on the surface. However, it did not have any consequences on the target integrity or the ^{135}La yield as the burnings were limited and the target material had not moved away from the proton beam. After 1 h irradiation at 20 μA, 55 MBq (2.75 MBq/μAh) of ^{135}La was produced at end-of-bombardment (EOB).

After irradiation, the silver around the target material showed some burnt discoloring (Fig. 1B). This hinted at the used target diameter being too small to take advantage of the whole beam diameter. We therefore prepared a target of similar composition, 1:2 $^{nat}BaCO_3$:Al (w/w), but pressed at 2.5 tons in a silver disc carved with a larger hole (Ø = 14 mm) in the center. The amount of target material was increased to 361 mg in order to maintain the same thickness as the target with a 9 mm diameter (Table 1, Target 2). The larger diameter of the target unfortunately led to a reduction of the heat dissipation capacity of the silver disc. After 1 h of irradiation at 20 μA, the target had suffered from overheating and was severely damaged (Fig. 1C). The Nb foil did not break but presented with a strong deformation due to the exposure to high temperature. The target material had turned black and crumbly. This might be due to a redox reaction between the Al and the CO_3^{-2} which would lead to the formation of Al_2O_3 and carbon compounds. The gain in activity from utilizing more of the beam was very limited with 65 MBq (3.25 MBq/μAh) of ^{135}La measured at EOB. Even if the target had been able to withstand the irradiation conditions, the gain in activity was only 18%, which was too small compared to the additional amount of target material used. The 9 mm diameter was therefore kept as preferred target size.

Another attempt to increase the production of ^{135}La was to use a target mixture with a larger $^{nat}BaCO_3$ content (Table 1, Target 3). A target consisting of 150 mg of a 1:1 $^{nat}BaCO_3$:Al (w/w) mixture and with a 9 mm diameter was irradiated for 1 h at 20 μA, which resulted in the target material becoming burned and crumbly after the irradiation (Fig. 1D). The amount of ^{135}La produced was 66 MBq (3.3 MBq/μAh) at EOB, which was higher than for the 150 mg 1:2 $^{nat}BaCO_3$:Al (w/w) target, which was 55 MBq (2.75 MBq/μAh) at EOB. Further studies with varying $^{nat}BaCO_3$:Al ratios were however not made due to the limited yield increase from the 1:2 to 1:1 ratio. The 1:2 $^{nat}BaCO_3$:Al (w/w) ratio was therefore kept as the favored target mixture ratio.

Table 1
Composition and ^{135}La yield of the tested $^{nat}BaCO_3$:Al targets. All targets were irradiated at 20 μA for 1.

	Target 1	Target 2	Target 3
Target diameter (mm)	9	14	9
Target mass (mg)	150	361	150
Target thickness (mg/cm^2)	236	235	236
$BaCO_3$/Al ratio (w/w)	1/2	1/2	1/1
Yield (MBq/μAh)	2.75	3.25	3.3

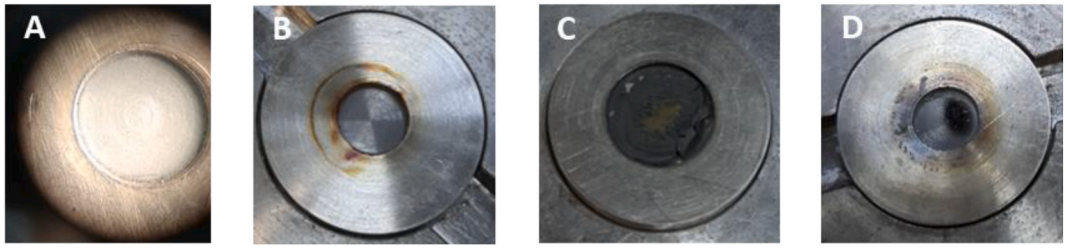

Fig. 1. Target compositions and irradiation. (**A**) Magnification of a 1:2 $^{nat}BaCO_3$:Al (w/w) target (Ø = 9 mm) pressed in a silver disc, before irradiation. (**B**) The same target as 1A, after irradiation. (**C**) A 1:2 $^{nat}BaCO_3$:Al (w/w) target (Ø = 14 mm) pressed in a silver disc, after irradiation. (**D**) A 1:1 $^{nat}BaCO_3$:Al (w/w) target (Ø = 9 mm) pressed in a silver disc, after irradiation.

After irradiation, the targets were dissolved at 60 °C in aq. HCl (3 M, 7–10 mL). Analysis by gamma spectroscopy 20–22 h after EOB, showed that the main radionuclides produced were: ^{132}La, ^{133}La, ^{135}La, ^{135m}Ba, and ^{132}Cs, the latter possibly originating from the ^{135}Ba(p,α)^{132}Cs nuclear reaction. In addition to those, radionuclides produced from impurities in the target material and from the silver backing material could also be identified: ^{107}Cd originating from the silver disc, ^{56}Co from the presence of an iron (Fe) impurity in the Al powder, and $^{86,\ 87,\ 87m,\ 88}$Y from a strontium (Sr) impurity in $^{nat}BaCO_3$.

3.2. Theoretical yield calculations

When using $^{nat}BaCO_3$ as target material and irradiating with a 16.5 MeV proton beam, two nuclear reactions contribute to the ^{135}La production: ^{135}Ba(p,n)^{135}La and ^{136}Ba(p,2n)^{135}La. Enriched [^{136}Ba]$BaCO_3$ could therefore also be a suitable starting material. In order to estimate the yields that could be achieved when using enriched [^{135}Ba]$BaCO_3$ and [^{136}Ba]$BaCO_3$ respectively, we performed theoretical yield calculations. Using SRIM software, we calculated the stopping power of successive layers of a 1:2 $^{nat}BaCO_3$:Al mixture, corresponding to the decreased beam energy in the layers from 16 MeV to 10 MeV. For each layer, the associated ^{nat}Ba cross-section for the (p,xn) reactions leading to the production of ^{135}La was taken from experimental cross-sections data published by Prescher and Tárkányi (Prescher et al., 1991; Tárkányi et al., 2010). As a result, for our 9 mm diameter target (0.64 cm^2 area, 153 mg target material) and after 2 h irradiation at 20 μA with a 16 MeV proton beam, we obtained a theoretical yield of 170 MBq of ^{135}La. Experimentally, with those irradiation conditions and the stated composition, 102 MBq of ^{135}La at EOB was produced from a 150 mg target. A similar target pressed with an enriched [^{135}Ba]$BaCO_3$:Al 1:2 mixture (152 mg) produced 811 MBq at EOB of ^{135}La. The natural abundance of ^{135}Ba is 6.6 % and the isotopic enrichment of the [^{135}Ba]$BaCO_3$ used for the experiment was 94.9 %. If ^{135}La was produced only from the ^{135}Ba(p,n)^{135}La nuclear reaction when using $^{nat}BaCO_3$, the estimated produced activity at EOB from [^{135}Ba]$BaCO_3$ would be 1469 MBq. As only 811 MBq was produced from the target containing enriched [^{135}Ba]$BaCO_3$, it is assumed that around 55 % of ^{135}La was produced by the ^{135}Ba(p,n)^{135}La nuclear reaction and thus 45 % of ^{135}La was produced from the ^{136}Ba(p,2n)^{135}La nuclear reaction when using $^{nat}BaCO_3$ as target material. It is important to note that these values are to be taken with caution. They are most likely underestimating the proportion of activity coming from the ^{135}Ba(p,n)^{135}La reaction, since the calculations assume that no ^{135}La is produced when the beam energy is below 8 MeV. This is due to the lack of experimental cross-section data below 11.9 MeV. In reality, the ^{135}Ba(p,n)^{135}La reaction likely keeps occurring down to 6–7 MeV as suggested by the calculated cross-sections reported by Nelson et al. (2020). Our calculations therefore also show that 150 mg of target material in a 9 mm diameter disc is not sufficient to have a "thick target". 153 mg of target material has only enough stopping power to reduce the proton beam energy down to 10 MeV, leaving some of the beam energy unused for ^{135}La production. To verify that, we prepared new targets with 200 mg target material for the high activity ^{135}La production which would have enough stopping power to reduce the proton beam energy to 7 MeV. The 200 mg target seemed to have similar beam current tolerance as the 150 mg target as it stayed intact at a beam current of 20 μA. This resulted in an increase in ^{135}La produced from 1.46 ± 0.11 GBq (18 ± 1 MBq/μAh) (150 mg target, n = 6) to 1.62 ± 0.18 GBq (20 ± 2 MBq/μAh) (200 mg target, n = 5) decay corrected to EOB, which is consistent with the calculations.

From the comparison between our calculations and the corresponding experiments, it appears that $^{135}BaCO_3$ is a more suitable target material than $^{136}BaCO_3$ for the production of ^{135}La. Theoretical calculations performed by Jastrzebski et al. for 100 % enriched ^{135}Ba and ^{136}Ba also indicate that the ^{135}Ba(p,n)^{135}La reaction will result in a higher production yield than the ^{136}Ba(p,2n)^{135}La reaction at proton energies from 5 to 16 MeV (Jastrzębski et al., 2020). In addition to an equal or even better production yield when using $^{135}BaCO_3$, the p,n reaction is also expected to produce the cleanest outcome. A more energetic reaction such as p,2n will result in an increased ^{135}La yield when using protons with energies from 35 MeV to 12 MeV, but has a higher probability of forming undesired radioactive byproducts and requires a proton beam of higher energy.

3.3. ^{135}La purification procedure

The purification procedure was developed for a 150–200 mg 1:2 $BaCO_3$:Al (w/w) target. A summary of the purification procedure can be seen in Scheme 1. The target was first dissolved at 60 °C in aq. HCl (3 M). It was not possible to dissolve $BaCO_3$ in concentrated HCl and aq. HCl (3 M) was chosen to dissolve the target. The solution was then evaporated to dryness in order to minimize the volume of the solution loaded on the column. After evaporation of the aq. HCl to dryness, the solid was redissolved in a few mL of aq. HCl (0.01 M). Addition of aq. HCl (30 %, w/w) in order to reach an HCl concentration of around 8 M, led to the precipitation of most of the Ba in the form of $BaCl_2$. The precipitate was removed by centrifugation and stored separately for recycling. 93 ± 5 % (n = 16) of the radionuclidic impurity ^{135m}Ba was removed in this way.

As part of the purification procedure optimization, we first deployed two successive columns to remove Al as well as trace metal impurities (essentially Fe and zinc (Zn)). In order to shorten the procedure as much as possible, we developed a single column (1 mL volume) packed with tandem layers of the two resins: a layer of TrisKem DGA resin (branched, 300 mg) on top and TK200 resin (100 mg) at the bottom. The use of a single column with DGA resin for the separation of ^{135}La from Ba has previously been reported where the target was dissolved in aq. HNO_3 and loaded on the column (Abel et al., 2018; Aluicio-Sarduy et al., 2019, 2020; Nelson et al., 2020, 2022). Silver discs were used as the target backing in our experiments which excluded the use of HNO_3 to dissolve the target. A separation procedure with aq. HCl was therefore developed. The DGA resin was found to efficiently retain the La and let the Al and Ba pass through with aq. HCl (8 M) as eluent. DGA resin is however not suitable for removing impurities such as Fe and Zn that tend to partially co-elute with La when using HCl as eluent (Pourmand and Dauphas, 2010). The TK200 resin is reported by the manufacturer to

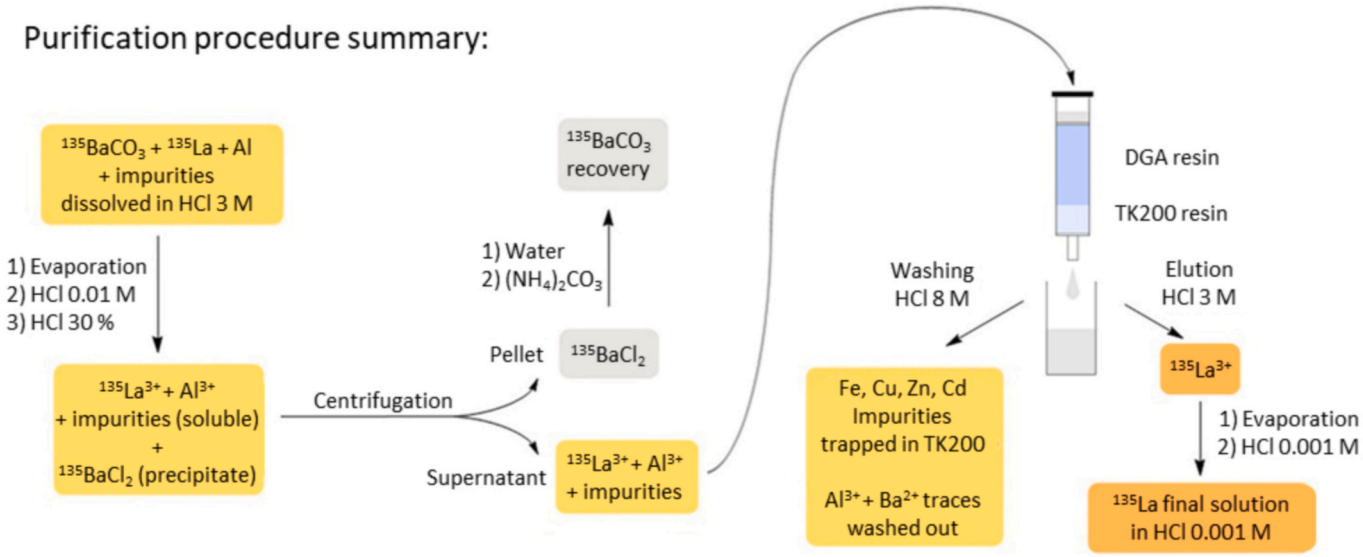

Scheme 1. Schematic overview of the procedure used for purification of ^{135}La from irradiated [^{135}Ba]$BaCO_3$:Al targets.

retain Fe and Zn when aq. HCl (3 M) is used as eluent (TRISKEM, 2017). Since La can be eluted with aq. HCl concentrations of 3 M and lower, the combination of both resins created a suitable column for ^{135}La purification. With this column, Al and Ba were washed out first in aq. HCl (8 M), and trace impurities were retained during the elution of La with aq. HCl (3 M).

After removal of the Ba precipitate, the supernatant was loaded on the combined column described above, which had previously been washed with aq. HCl (3 M) and conditioned with aq. HCl (8 M). The column was then washed with aq. HCl (8 M) to remove Ba and Al, followed by elution of the ^{135}La with aq. HCl (3 M). The elution profile for ^{135}La and ^{135m}Ba can be seen in Fig. 2. The eluate was evaporated to dryness and redissolved in aq. HCl (0.001 M), making it ready for radiolabeling. The overall recovery of ^{135}La was 97.2 ± 3.6 %, decay corrected (n = 13).

The stable element impurities in the final product from the first three batches was measured by ICP-OES analysis. We saw primarily traces of La (1.4 ± 0.04 nmol) and Ba (1.6 ± 1.5 nmol) and 78.3 ± 45.1 nmol Al (n = 3). The gamma spectrum at 21 h after EOB of the purified sample from a 150 mg 1:2 $^{nat}BaCO_3$:Al (w/w) target, which had been irradiated for 2 h at 20 μA showed the presence of three La isotopes, 0.15 ± 0.004 MBq ^{132}La, 0.87 ± 0.04 MBq ^{133}La, and 44.2 ± 0.76 MBq ^{135}La, as well as 0.045 ± 0.002 MBq ^{56}Co, likely originating from an Fe impurity in the Al powder. This radionuclidic impurity was not removed by our purification procedure (Fig. 3A).

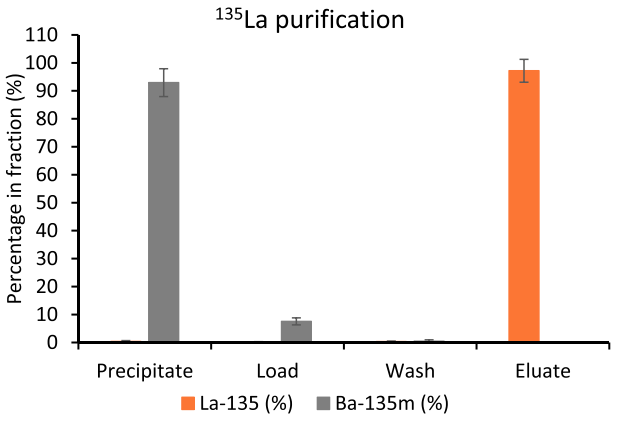

Fig. 2. The percentage of ^{135}La and ^{135m}Ba in the precipitate and in the different fractions from the purification process.

3.4. *High activity ^{135}La production with [^{135}Ba]$BaCO_3$:Al target*

The production procedure optimized with $^{nat}BaCO_3$ as starting material was applied to the production of ^{135}La from enriched [^{135}Ba]$BaCO_3$. The $BaCO_3$:Al ratio was kept as 1:2 (w/w). As the aim was to demonstrate a comparatively high ^{135}La yield of more than 1 GBq, the target was irradiated for 4 h. The ^{135}Ba-enriched target limited the formation of multiple La radioisotopes to negligible levels. The target could therefore be handled and worked up already 30 min after EOB. The only contaminant radionuclides detected besides ^{135}La were ^{135m}Ba, ^{107}Cd, ^{132}Cs, and ^{56}Co. The activity produced at EOB reached 1.46 ± 0.11 GBq (18 ± 1 MBq/μAh, 150 mg target, n = 6) to 1.62 ± 0.18 GBq (20 ± 2 MBq/μAh, 200 mg target, n = 5). This corresponded to saturation yields of 10.70 ± 0.80 GBq (or 535 ± 40 MBq/μA) and 11.91 ± 1.31 GBq (or 596 ± 66 MBq/μA), respectively. After dissolution in aq. HCl (3 M) followed by evaporation to dryness, the solid was redissolved in aq. HCl (0.01 M). Addition of aq. HCl (30% (w/w)) led to the precipitation of most of the ^{135}Ba in the form of [^{135}Ba]$BaCl_2$. After centrifugation, followed by washing, the supernatant was loaded on a column packed with DGA resin on the top and TK200 resin at the bottom washed with aq. HCl (3 M) and conditioned with aq. HCl (8 M) prior to loading. The loaded column was first washed with aq. HCl (8 M), and the ^{135}La was then eluted with aq. HCl (3 M). After evaporation to dryness, the eluate was redissolved in aq. HCl (0.001 M). ICP-OES measurement showed that the procedure gave a high purity [^{135}La]$LaCl_3$ solution both with a 150 mg and 200 mg target. The total amount of impurities detected in the full batch (n = 11) were 37.4 ± 17.5 nmol Al, 0.3 ± 0.2 nmol Ba, 1.3 ± 2.5 nmol Fe, 1.1 ± 2.9 nmol Zn, and 1.3 ± 0.3 nmol La, which corresponded to a decay corrected molar activity of 1277 ± 383 MBq/nmol (150 mg target, n = 6) and 1119 ± 50 MBq/nmol (200 mg target, n = 3) and a decay corrected apparent molar activity of 28.4 ± 10.1 MBq/nmol (150 mg target, n = 6) and 86.5 ± 39.5 MBq/nmol (200 mg target, n = 3). The Ba/La separation factor was $5•10^7$ ± $4•10^7$ for the 150 mg target and $6•10^7$ ± $5•10^7$ for the 200 mg target and the Al/La separation factor was $3•10^6$ ± $2•10^6$ for the 150 mg target and $5•10^6$ ± $3•10^6$ for the 200 mg target.

The [^{135}Ba]$BaCl_2$ could be recycled and converted back to [^{135}Ba]$BaCO_3$ by dissolution in a few mL of water and addition of $(NH_4)_2CO_3$. After centrifugation and thorough drying, the precipitated [^{135}Ba]$BaCO_3$ could be used to prepare a new target.

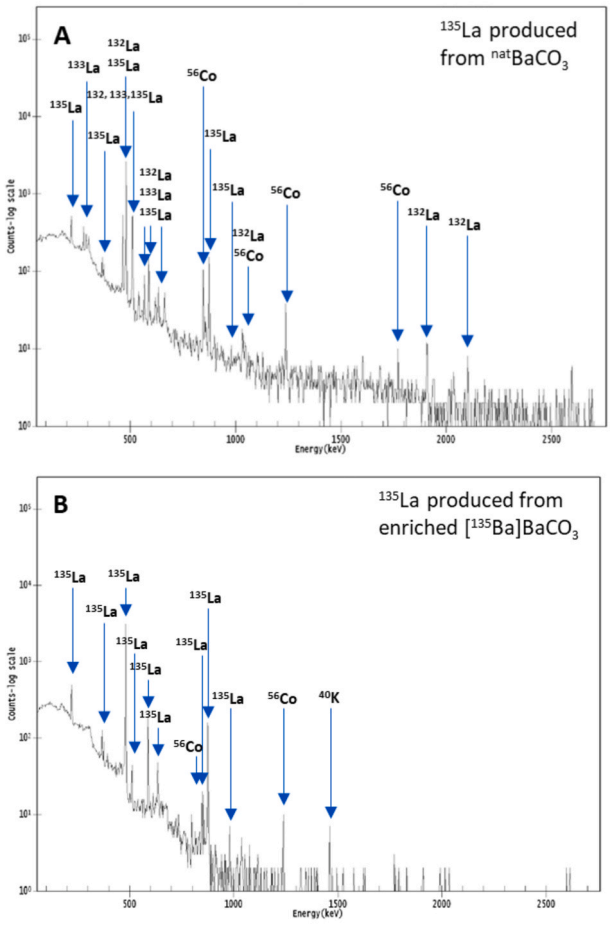

Radio-nuclide	γ lines, keV
^{132}La	465, 480, 511, 516, 540, 567, 663, 1032, 1037, 1047, 1910, 2102
^{133}La	279, 290, 302, 511, 567, 618, 622
^{135}La	221, 367, 375, 481, 511, 588, 634, 875, 980
^{56}Co	847, 1038, 1238, 1771
^{40}K	1461

Fig. 3. Gamma spectroscopic characterization of ^{135}La from different targets. (**A**) Gamma spectrum of ^{135}La when produced from ^{nat}BaCO$_3$, 21 h after EOB. (**B**) Gamma spectrum of ^{135}La when produced from enriched [^{135}Ba]BaCO$_3$, 22 h after EOB. The corresponding γ lines energies are given below the spectra.

Apart from the increased ^{135}La production yield, the enriched [^{135}Ba]BaCO$_3$ target material allowed for a much higher radionuclidic purity (RNP). ^{135}La is the only La isotope detected in the final sample, with ^{56}Co present as a minor impurity (81 ± 36 kBq (150 mg target, n = 6) and 103 ± 20 kBq (200 mg target, n = 5)) (Fig. 3B). The ^{56}Co likely originated from an Fe impurity present in the Al powder. It can therefore potentially be avoided by using an Al powder of higher purity.

3.5. Effective molar activity determination

To confirm the apparent molar activity determined from the ICP-OES results, we measured the effective molar activity of the final ^{135}La samples. Titrations were done using the chelators DOTA, diethylenetriaminepentaacetic acid (DTPA) and CHX-A″-DTPA ([(*R*)-2-Amino-3-(4-nitrophenyl)propyl]-trans-(*S*,*S*)-cyclohexane-1,2-diamine-pentaacetic acid (*p*-NO$_2$-Bn-CHX-A″-DTPA)), which are known to form stable complexes with lanthanides (Byegård et al., 1999; Viola-Villegas and Doyle, 2009; Pandey et al., 2017). The labeling of DTPA and CHX-A″-DTPA could be performed at room temperature, while the labeling of DOTA was performed at 90 °C. An example of the formation of the ^{135}La-complexes as a function of chelator added can be seen in Fig. 4. The effective molar activity was calculated from the points with less than 100 % complex formation. The amount of competing metals was calculated by dividing the amount of chelator added with the fraction of complex formed. The effective molar activity was calculated by dividing the ^{135}La activity with the amount of competing metals.

The DOTA titration showed the herein described methodology to produce samples with a decay corrected effective molar activity of 57.7 ± 15.3 MBq/nmol (150 mg target, n = 3) and 79.6 ± 25.3 MBq/nmol (200 mg target, n = 4). The titration with DTPA gave similar results with a decay corrected effective molar activity of 104.0 ± 40.4 MBq/nmol (200 mg target, n = 2), while the titration with CHX-A″-DTPA gave a higher effective molar activity of 186.5 ± 83.8 MBq/nmol (200 mg target, n = 2). The same ^{135}La batch was used for both of the two titrations with DTPA and CHX-A″-DTPA. The same ^{135}La batch was used for two of the titrations with DOTA and the average of these titrations was 92.7 ± 9.1 MBq/nmol, so this ^{135}La batch was of slightly higher purity than the average ^{135}La batch. The effective molar activity from the CHX-A″-DTPA titrations was however still higher than for the DOTA and DTPA titrations, which indicated that the labeling of CHX-A″-DTPA was less affected by the metal impurities than the labeling of DOTA and DTPA. The main metal impurity in the ^{135}La batches according to ICP-OES was Al, but even when Al was present in concentrations higher than that of the chelator during the titration, a full chelation of La could still be obtained in most cases. This indicated that the presence of Al only affected the labeling to some low extent and the effective molar activity values demonstrate that the ^{135}La purified with our method is suitable for labeling.

3.6. Serum stability of ^{135}La-DOTA, ^{135}La-DTPA and ^{135}La-CHX-A″-DTPA

Having in mind the potential future applications of ^{135}La-DOTA, ^{135}La-DTPA and ^{135}La-CHX-A″-DTPA derivatives for AeRT, we investigated the serum stability of the ^{135}La-DOTA, ^{135}La-DTPA and ^{135}La-CHX-A″-DTPA complexes over two days (Fig. 5). Mixtures containing each ^{135}La complex and mouse serum were incubated at 37 °C. The mixtures were analyzed by radio-TLC after 0, 3, 18, 24, 42, and 48 h to quantify the percentage of the ^{135}La-complexes over time. During the

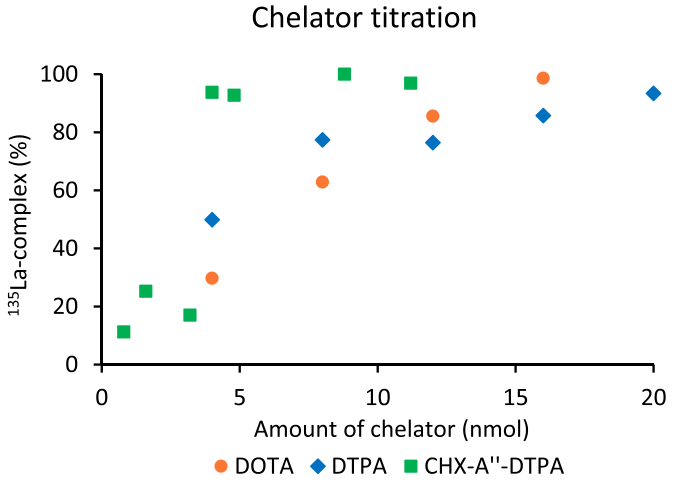

Fig. 4. Example of the chelator titration for one of the ^{135}La batches with DOTA, DTPA and CHX-A″-DTPA. The amount of chelator was normalized to the full ^{135}La-batch.

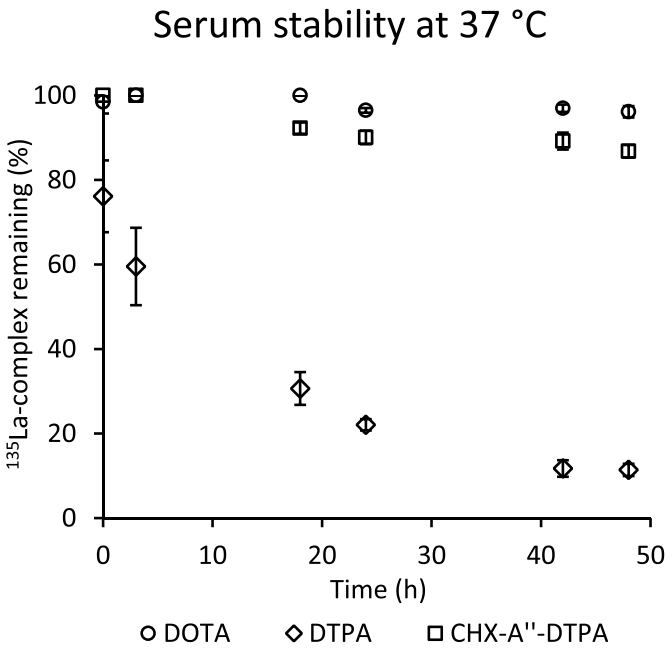

Fig. 5. Serum stability of free ^{135}La complexes. The percentage of intact ^{135}La-DOTA, ^{135}La-DTPA, and ^{135}La-CHX-A″-DTPA complex in mouse serum at 37 °C after 0, 3, 18, 24, 42 and 48 h. Error is shown as standard deviation (n = 3).

stability study ^{135}La-species with retention factors (R_f) of 0 started to form, presumably due to instability of the complexes in serum. The amount of ^{135}La-DTPA complex decreased rapidly, and the percentage of the intact complex was already decreased to 76% immediately upon mixing with serum. At the end of the study the remaining ^{135}La-DTPA complex was around 10%. The stability of the ^{135}La-DOTA and ^{135}La-CHX-A″-DTPA complexes was higher than the ^{135}La-DTPA complex with 96% and 87% intact complex after 48 h, respectively.

4. Discussion

Pressed $BaCO_3$/Al targets were suitable for the production of ^{135}La with a 16.5 MeV cyclotron. The content of Al used for the target made it possible to irradiate $BaCO_3$ at 20 μA, which is higher than previously reported, to our knowledge (Mansel and Franke, 2015; Jastrzębski et al., 2020; Chakravarty et al., 2022; Nelson et al., 2022). This increased current was enabled by the high thermal conductivity of Al. The Al powder was also necessary in order to press the $BaCO_3$ in a cylindrical recession machined into a silver disc target backing. The presence of Al in the target did not lead to the production of long-lived radionuclides and Al is a light element with a low stopping of the proton beam.

It would be advantageous to increase the content of $BaCO_3$ in the target in order to obtain higher ^{135}La production yields. In our cyclotron settings, a ratio of 1:1 between $BaCO_3$/Al did lead to the target being burned and crumbly after 1 h irradiation at 20 μA. The expected yield increase was 38 % for a 200 mg target with [^{135}Ba]$BaCO_3$ when going to a ratio of 1:1 from 1:2, but as some burnings were observed already on 1:2 $BaCO_3$:Al targets if the pressing was imperfect, it was expected that the ratio could only be increased slightly and it was not tested if a target with a $BaCO_3$:Al ratio between 1:2 and 1:1 was stable. In order to use targets with a higher $BaCO_3$:Al ratio, a lower current could be used or the target cooling during the irradiation could be improved. Our target was water-cooled on the back of the silver disc, but helium-cooling on the Nb front foil could be implemented to improve the cooling.

The ^{135}La yield was increased by a factor of 8 by going from $^{nat}BaCO_3$ to [^{135}Ba]$BaCO_3$. Due to the contribution from the (p,2n) reaction on ^{136}Ba when using $^{nat}BaCO_3$, the increase was less than first expected. With our target composition and purification method, the RNP at end of purification was improved from 98% (purification one day after production) to >99.9% (purification directly after production). As both the production yield and the RNP could be improved by using enriched [^{135}Ba]$BaCO_3$ and the fact that the material can be reused, compensate for the higher cost of the enriched material. Stopping power values from SRIM software were used to calculate the theoretical yield. No experimental cross section data for the ^{135}Ba(p,n)^{135}La nuclear reaction could be found on EXFOR, so the calculated cross section from Nelson and coworkers were used for the calculation (Nelson et al., 2020). The produced yield was 88.2 ± 1.0 % of the theoretical yield. The use of the $BaCO_3$:Al target results in a lower ^{135}La production compared to a metallic Ba target with the same thickness due to the lower amount of Ba in the mixed target. The $BaCO_3$:Al target is not as sensitive to air and moisture as the metallic Ba target and the access to enriched [^{135}Ba]$BaCO_3$ makes the use of $BaCO_3$ as target material advantageous.

The purification procedure could be performed within 4 h, where the dissolution of the target and the following evaporation to dryness were the most time-consuming steps. The actual purification step was fast and efficient as the DGA resin and the TK200 resin were combined in one column. The purification procedure was suitable both for 150 mg and 200 mg targets. The amount of DGA and TK200 resin was not optimized and less resin might be used with similar separation efficiency. As Ba and Al have no or very low binding to the DGA resin and TK200 resin (Pourmand and Dauphas, 2010; TRISKEM, 2017) at high HCl concentration, the washing step is relatively short. 3 M HCl was chosen for the elution of La because Fe has a high binding to the DGA resin and the TK200 resin at 3 M HCl. Zn has a high binding to the TK200 resin at HCl concentrations above 1 M. It was possible to retain Fe and Zn, which are common impurities in the production of ^{135}La, on the resin by using 3 M HCl. The eluate needs to be evaporated to dryness and redissolved in a less acidic solution in order to be compatible with common labeling procedures and it is not possible to elute La with a less acidic solution without co-eluting Fe and Zn impurities.

An attempt to shortening the purification procedure could be to omit the first evaporation step and add concentrated HCl directly to the dissolved target mixture. It is however necessary to reach an HCl concentration around 8 M before loading on the column to ensure a high binding of La to the DGA resin. The volume of aq. HCl (3 M) needed to dissolve the target was 9–11 mL and the HCl concentration decreases during the dissolving of the target. It will thus require a relatively large volume of concentrated HCl to reach 8 M and the loading of the solution on the column will take longer time.

The labelling of the three chelators DOTA, DTPA, and CHX-A″-DTPA and the stability of the ^{135}La-complexes in serum were consistent with the chemical structure of the chelators. DOTA is a macrocyclic chelator, which often has a higher kinetic inertness than acyclic chelators as DTPA and CHX-A″-DTPA. CHX-A″-DTPA has a more rigid structure and is more kinetically inert compared to DTPA (Price and Orvig, 2014). DOTA is a suitable chelator for ^{135}La, if DOTA is conjugated to a targeting vector, which can withstand high labeling temperatures. The ^{135}La-DOTA complex was in our experiment the most stable of the three complexes in serum with around 96% intact complex after 48 h. If targeting vectors which are not stable at high temperatures, e.g. antibodies, were to be used, then CHX-A″-DTPA chelator seems to be more suitable, as the labeling with ^{135}La can be performed at room temperature and the stability of the ^{135}La-CHX-A″-DTPA complex in serum was still relatively high (87%) after 48 h. Furthermore, the CHX-A″-DTPA chelator seemed to be less affected by the metal impurities as a higher effective molar activity was observed with this chelator compared to DOTA and DTPA. The labeling with DTPA could be performed at room temperature as with CHX-A″-DTPA, but the ^{135}La-DTPA complex was substantially less stable in serum as only 30% of intact complex was present after 18 h, which is around one half-life of ^{135}La, and it is assumed that the stability of the ^{135}La-DTPA will not be sufficient for *in vivo* application.

The effective molar activities determined from the titrations with DTPA and CHX-A″-DTPA was higher than the apparent molar activity

measured by ICP-OES, which indicates that the labeling of these two chelators is less affected by the presence of Al, since full chelation of ^{135}La could be obtained even when Al was present in concentrations higher than that of the chelator during the titration. The effective molar activity values of the DOTA titrations were closer to the apparent molar activity values measured by ICP-OES. This indicates that the presence of Al affects the labeling of DOTA more than for DTPA and CHX-A″-DTPA. It was however possible to obtain full chelation of ^{135}La with DOTA in most cases with DOTA concentrations lower than the concentration of Al. It is thus assumed that Al is a less critical impurity than Zn and Fe in terms of labeling efficiency. The amount of Al should only be kept low to prevent potential toxicological effects, if the finished labeled compound is injected without further purification.

In our initial experiments we observed that the eluate from the DGA/TK200 column had a high purity, but that the following evaporation step could introduce impurities such as Fe, Zn, and Al. The evaporation was therefore performed in a capped, acid-washed vial with an argon inlet and an outlet tubing inserted in the cap, which made it possible to obtain the final ^{135}La in a higher purity.

The amount of stable La at the end of purification was 1.3 ± 0.3 nmol and is expected to derive from the [^{135}Ba]$BaCO_3$. By using recovered [^{135}Ba]$BaCO_3$ the amount of La might be lower due to the separation of Ba and La in the precipitation step. This would result in a higher molar activity. Furthermore, the molar activity can be increased if higher ^{135}La activities are produced, e.g. with longer irradiation time or higher current.

The quality and the yield of ^{135}La produced in these settings are likely to be sufficient for *in vitro* and *in vivo* efficacy studies, but an upscaled production would be needed for clinical studies. The advantages of ^{135}La compared to other promising Auger electron emitters, e.g. cobalt-58m (^{58m}Co), antimony-119 (^{119}Sb), and erbium-165 (^{165}Er), are the relative easy separation of the radionuclide and the target material, the suitable decay characteristics, such as a half-life of around 19 h and decay to a stable daughter, and the possibility of using well-established DOTA for radiolabeling targeting vectors. ^{58m}Co has a shorter half-life of 9.1 h and decays to ^{58g}Co, which has a long half-life of 70.9 d, but can nonetheless be produced in very large activity yields. Enriched [^{58}Fe]Fe is needed for high activity ^{58m}Co productions but the natural abundance of ^{58}Fe is low (0.3 %). The advantages of ^{58m}Co are that the separation of the radionuclide and the target material is well-described and ^{58m}Co can also be chelated by DOTA, as well as NOTA (Barrett et al., 2021). ^{119}Sb has a longer half-life of 38.2 h and suitable decay characteristics. Enriched tin-119 ([^{119}Sn]Sn) is needed for high activity production, and the separation of ^{119}Sb and Sn is possible with ion exchange chromatography or liquid-liquid extraction. The chelation of ^{119}Sb is challenging however and still under development (Randhawa et al., 2021). ^{165}Er is another promising Auger emitter with a suitable half-life of 10.4 h ^{165}Er can be produced from monoisotopic holmium (Ho), so an enriched target material is not needed. The separation of ^{165}Er and Ho is challenging however, as these are two neighboring lanthanides with similar chemical properties (Gracheva et al., 2020). Even more promising Auger electron emitters exists, besides those mentioned here, which all have different advantages and challenges, and with its suitable decay and chemical properties ^{135}La is among those candidates (Filosofov et al., 2021).

5. Conclusion

A novel cyclotron target composition of an enriched [^{135}Ba]$BaCO_3$:Al mixture for the production of ^{135}La was developed. The target is more stable than conventional pressed metallic Ba targets and has better thermal conductivity compared to pure $BaCO_3$. After 4 h of irradiation with a 16.5 MeV proton beam and 20 μA current, 1.62 ± 0.18 GBq (20 ± 2 MBq/μAh, n = 5, 200 mg [^{135}Ba]$BaCO_3$:Al 1:2 (w/w) target) was produced, corresponding to a saturation yield of 11.91 ± 1.31 GBq (or 596 ± 66 MBq/μA). In order to deal with the high amount of Al filling, we developed an efficient purification procedure, comprising a precipitation step followed by a single column purification that yielded a high purity [^{135}La]$LaCl_3$ solution. The precipitation step allowed for recycling of the valuable enriched [^{135}Ba]$BaCO_3$ which makes the overall procedure very cost efficient. The final [^{135}La]$LaCl_3$ solution could be used for the labeling of the DOTA, DTPA and CHX-A″-DTPA chelators and a stability study in serum showed high stability of the ^{135}La-DOTA and ^{135}La-CHX-A″-DTPA complexes, while the ^{135}La-DTPA complex had limited stability. The overall procedure for the production and purification of ^{135}La was robust and reliable, which opens up for new possibilities for high activity productions of ^{135}La and further research into the therapeutic efficacy of ^{135}La.

Funding

The project has received funding from the European Union's Horizon 2020 research and innovation programme under grant agreement No 101008571 (PRISMAP – The European medical radionuclides programme) and from The Innovation Fund Denmark under grant agreement No 1046-00027 within the InnoExplorer programme.

CRediT authorship contribution statement

Kristina Søborg Pedersen: Writing – review & editing, Writing – original draft, Methodology, Investigation, Formal analysis. **Claire Deville:** Writing – original draft, Methodology, Investigation, Formal analysis. **Ursula Søndergaard:** Writing – review & editing, Investigation, Formal analysis. **Mikael Jensen:** Writing – review & editing, Supervision, Funding acquisition, Formal analysis, Conceptualization. **Andreas I. Jensen:** Writing – review & editing, Supervision, Funding acquisition, Conceptualization.

Declaration of competing interest

The authors declare the following financial interests/personal relationships which may be considered as potential competing interests:

Andreas I. Jensen reports financial support was provided by The Innovation Fund Denmark. Mikael Jensen reports financial support was provided by European Union Horizon 2020 research and innovation programme. Claire Deville reports financial support was provided by The Innovation Fund Denmark. Kristina Soeborg Pedersen reports financial support was provided by The Innovation Fund Denmark. Kristina Soeborg Pedersen has patent #EP22182651.4 pending to Technical University of Denmark. Claire Deville has patent #EP22182651.4 pending to Technical University of Denmark. Andreas I. Jensen has patent #EP22182651.4 pending to Technical University of Denmark. Mikael Jensen has patent #EP22182651.4 pending to Technical University of Denmark.

Data availability

Data will be made available on request.

References

Abel, E.P., Clause, H.K., Fonslet, J., Nickels, R.J., Severin, G.W., 2018. Half-lives of 132La and 135La. Phys. Rev. C 97 (3), 034312. https://doi.org/10.1103/PhysRevC.97.034312.

Aluicio-Sarduy, E., Hernandez, R., Olson, A.P., Barnhart, T.E., Cai, W., Ellison, P.A., Engle, J.W., 2019. Production and in vivo PET/CT imaging of the theranostic pair 132/135La. Sci. Rep. 9, 1–6. https://doi.org/10.1038/s41598-019-47137-0, 10658.

Aluicio-Sarduy, E., Thiele, N.A., Martin, K.E., Vaughn, B.A., Devaraj, J., Olson, A.P., Barnhart, T.E., Wilson, J.J., Boros, E., Engle, J.W., 2020. Establishing radiolanthanum chemistry for targeted nuclear medicine applications. Chem. Eur J. 26 (6), 1238–1242. https://doi.org/10.1002/chem.201905202.

Álvarez, N.H., Bauer, D., Hernández-Gil, J., Lewis, J.S., 2021. Recent advances in radiometals for combined imaging and therapy in cancer. ChemMedChem 16 (19), 2909–2941. https://doi.org/10.1002/cmdc.202100135.

Barrett, K.E., Houson, H.A., Lin, W., Lapi, S.E., Engle, J.W., 2021. Production, purification, and applications of a potential theranostic pair: cobalt-55 and cobalt-58m. Diagnostics 11 (7), 1–27. https://doi.org/10.3390/diagnostics11071235, 1235.

Buchegger, F., Perillo-Adamer, F., Dupertuis, Y.M., Delaloye, A.B., 2006. Auger radiation targeted into DNA: a therapy perspective. Eur. J. Nucl. Med. Mol. Imag. 33 (11), 1352–1363. https://doi.org/10.1007/s00259-006-0187-2.

Byegård, J., Skarnemark, G., Skålberg, M., 1999. The stability of some metal EDTA, DTPA and DOTA complexes: application as tracers in groundwater studies. J. Radioanal. Nucl. Chem. 241 (2), 281–290. https://doi.org/10.1007/BF02347463.

Chakravarty, R., Patra, S., Jagadeesan, K.C., Thakare, S.V., Chakraborty, S., 2022. Electrochemical separation of 132/135La theranostic pair from proton irradiated Ba target', *Separation and Purification Technology*. Elsevier B.V. 280 (3), 119908 https://doi.org/10.1016/j.seppur.2021.119908.

Filosofov, D., Kurakina, E., Radchenko, V., 2021. 'Potent Candidates for Targeted Auger Therapy: Production and Radiochemical Considerations', *Nuclear Medicine and Biology*, vols. 94–95. Elsevier Inc., pp. 1–19. https://doi.org/10.1016/j.nucmedbio.2020.12.001

Fonslet, J., Tran, T.A., Lee, B.Q., Siikanen, J., Larsson, E., Kibédi, T., Stuchbery, A.E., Elema, D.R., Severin, G.W., 2015. 135La for Auger-based therapy: preparation, imaging and emission. J. Label. Compd. Radiopharm. 58, S24.

Fonslet, J., Lee, B.Q., Tran, T.A., Siragusa, M., Jensen, M., Kibédi, T., Stuchbery, A.E., Severin, G.W., 2018. 135La as an Auger-electron emitter for targeted internal radiotherapy. Phys. Med. Biol. 63, 015026 https://doi.org/10.1088/1361-6560/aa9b44.

Gracheva, N., Carzaniga, T.S., Schibli, R., Braccini, S., van der Meulen, N.P., 2020. ^{165}Er: a new candidate for Auger electron therapy and its possible cyclotron production from natural holmium targets. Appl. Radiat. Isot. 159, 1–8. https://doi.org/10.1016/j.apradiso.2020.109079, 109079.

Jastrzębski, J., Zandi, N., Choiński, J., Sitarz, M., Stolarz, A., Trzcińska, A., Vagheian, M., 2020. Investigation of the production of the auger electron emitter 135La using medical cyclotrons. Acta Phys. Pol. B 51 (3), 861–866. https://doi.org/10.5506/APhysPolB.51.861.

Ku, A., Facca, V.J., Cai, Z., Reilly, R.M., 2019. Auger electrons for cancer therapy – a review', *EJNMMI Radiopharmacy and Chemistry*. EJNMMI Radiopharm. Chem. 4 (27), 1–36. https://doi.org/10.1186/s41181-019-0075-2.

Mansel, A., Franke, K., 2015. Production of no-carrier-added 135La at an 18 MeV cyclotron and its purification for investigations at a concentration range down to 10â-15 mol/L. Radiochim. Acta 103 (11), 759–763. https://doi.org/10.1515/ract-2015-2427.

Nelson, B.J.B., Wilson, J., Andersson, J.D., Wuest, F., 2020. High yield cyclotron production of a novel 133/135La theranostic pair for nuclear medicine. Sci. Rep. 10 (1), 1–10. https://doi.org/10.1038/s41598-020-79198-x. Nature Publishing Group UK.

Nelson, B.J.B., Ferguson, S., Wuest, M., Wilson, J., Duke, M.J.M., Richter, S., Soenke-Jans, H., Andersson, J.D., Juengling, F., Wuest, F., 2022. First in vivo and phantom imaging of cyclotron-produced 133La as a theranostic radionuclide for 225Ac and 135La. J. Nucl. Med. 63 (4), 584–590. https://doi.org/10.2967/jnumed.121.262459.

Nielsen, K.M., Jensen, M., 2021. Fast, efficient, one-step purification of cyclotron produced lanthanum-135 using HDEHP-based resin and dilute hydrochloric acid. Nucl. Med. Biol. 96–97 (S1), S18–S19. https://doi.org/10.1016/s0969-8051(21)00297-3. Elsevier B.V.

Pandey, U., Gamre, N., Lohar, S.P., Dash, A., 2017. A systematic study on the utility of CHX-A''-DTPA-NCS and NOTA-NCS as bifunctional chelators for 177Lu radiopharmaceuticals. Appl. Radiat. Isot. 127 (April), 1–6. https://doi.org/10.1016/j.apradiso.2017.04.028. Elsevier Ltd.

Pourmand, A., Dauphas, N., 2010. Distribution coefficients of 60 elements on TODGA resin: application to Ca, Lu, Hf, U and Th isotope geochemistry. Talanta 81 (3), 741–753. https://doi.org/10.1016/j.talanta.2010.01.008.

Prescher, K., Peiffer, F., Stueck, R., 1991. Thin-target cross sections of proton-induced reactions on barium and solar cosmic ray production rates of xenon-isotopes in lunar surface materials. Nucl. Instrum. Methods Phys. Res. B 53 (2), 105–121. https://doi.org/10.1016/0168-583X(91)95645-T.

Price, E.W., Orvig, C., 2014. Matching chelators to radiometals for radiopharmaceuticals. Chem. Soc. Rev. 43 (1), 260–290.

Randhawa, P., Olson, A.P., Chen, S., Gower-Fry, K.L., Hoehr, C., Engle, J.W., Ramogida, C.F., Radchenko, V., 2021. Meitner-Auger electron emitters for targeted radionuclide therapy: mercury-197m/g and antimony-119. Curr. Rad. 14 (4), 394–419. https://doi.org/10.2174/1874471014999210111201630.

Tárkányi, F., Ditrói, F., Király, B., Takács, S., Hermanne, A., Yamazaki, H., Baba, M., Mohammadi, A., Ignatyuk, A.V., 2010. Study of activation cross sections of proton induced reactions on barium: production of 131Ba -> 131Cs. Appl. Radiat. Isot. 68 (10), 1869–1877. https://doi.org/10.1016/j.apradiso.2010.03.010.

TRISKEM, 2017. PRODUCT SHEET TK200 resin. Available at: https://www.triskem-international.com/catalog/products/resins-and-accessories/tk200-resin/bl,product,423,0. (Accessed 9 June 2022).

Viola-Villegas, N., Doyle, R.P., 2009. The coordination chemistry of 1,4,7,10-tetraazacyclododecane-N,N′,N″,N‴-tetra acetic acid (H4DOTA): structural overview and analyses on structure-stability relationships. Coord. Chem. Rev. 253 (13–14), 1906–1925. https://doi.org/10.1016/j.ccr.2009.03.013.